ACS APPLIED MATERIALS & INTERFACES

Research Article

www.acsami.org

Starch Nanocrystal Stabilized Pickering Emulsion Polymerization for Nanocomposites with Improved Performance

Sihem Bel Haaj,[†] Wim Thielemans,*[,‡] Albert Magnin,[§] and Sami Boufi*[,†]

[†]Sfax Faculty of Science-LMSE, University of Sfax, BP 802, 3018 Sfax, Tunisia

[‡]KU Leuven, Campus Kortrijk, Etienne Sabbelaan 53, 8500 Kortrijk, Belgium

[§]Laboratoire Rhéologie et Procédés, Grenoble-INP, UJF Grenoble 1, UMR CNRS 5520, BP 53, 38041 Grenoble Cedex 9, France

ABSTRACT: Latex/starch nanocrystal (SNC) nanocomposite dispersions were successfully synthesized via a one-step surfactant-free Pickering emulsion polymerization route using SNC as the sole stabilizer. The effect of the SNC content, initiator type and comonomer on the particle size, colloidal stability, and film properties were investigated. Both HCl and H_2SO_4-hydrolysed starch nanocrystals, each bearing different surface charges, were used as Pickering emulsion stabilizing nanoparticles. SNCs from HCl hydrolysis were found to provide a better stabilization effect, giving rise to a polymer dispersion with a lower average particle size. The mechanistic aspects of the Pickering emulsion polymerization were also discussed. Nanocomposites formed by film-casting the polymer Pickering emulsions showed better mechanical properties and optical transparency than those obtained by blending the polymer emulsion with a nanocrystal dispersion, showing the one-pot route to nanocomposite precursors to be doubly advantageous. Therefore, this in situ polymerization technique not only facilitates the use of SNC nanoparticles, it also provides a valuable nanocomposite with enhanced mechanical properties and high transparency level.

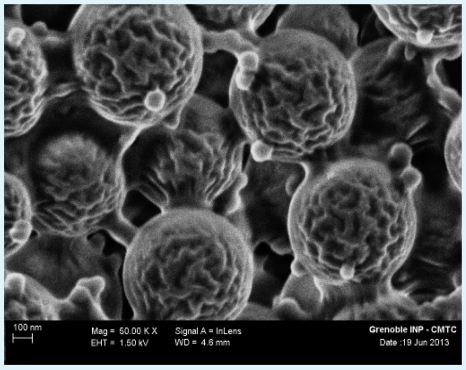

KEYWORDS: *Pickering, emulsion, starch nanocrystals, nanocomposite*

INTRODUCTION

Over the last two decades, in situ syntheses of nanocomposites via waterborne processes have gained increasing attention. For film-forming dispersions, a polymer emulsion also containing nanoparticles offers the advantage of having a single formulation ready for use in coating or adhesive applications. Preparation of this emulsion with the nanoparticles present (in situ approach) has the additional advantage of creating the formulation in one step when compared to the so-called ex situ approach, which requires the nanoparticles to be blended with the polymer latex after polymerization has taken place.

The in situ route reduces the necessary processing steps, avoids dilution and mixing phases, and also reduces the risk during manipulation of nanoparticles (NPs) as they are involved in fewer steps. Potential aggregation during processing further complicates work with polysaccharide-based NPs, where their strong tendency to self-aggregate prevents their delivery in the form of highly concentrated suspensions.

The presence of nanoparticles during emulsion polymerization might be further exploited to induce stabilization by what is known as Pickering stabilization. Using solid particles, conventional emulsifying agents can be omitted and hazardous surfactants may be replaced by less harmful materials and more environmentally-friendly components.[1] The use of surfactants is known to adversely affect the mechanical and water resistance properties of the resulting films,[2] making the Pickering polymerization approach of great interest.

In Pickering emulsions, solid particles of intermediate wettability with dimensions ranging from several nanometers to several micrometers attach to liquid−liquid interfaces and provide emulsion stability. The driving force for the stabilization process stems mainly from the Gibbs free energy penalty incurred by removing the adsorbed solid particles away from the interface.[3]

Recently, Pickering emulsion polymerization has been employed as a facile approach to design complex colloid-based structures. A wide range of inorganic particles, such as silica,[4] titania,[5] clay,[6,7] and carbon black[8] have been reported as Pickering emulsifiers.

On the other hand, polysaccharide-based nanoparticles such as cellulose nanocrystals, nanofibrillated cellulose and starch nanoparticles have emerged as one of the most promising renewable reinforcing nanofillers.[9,10] These NPs open the way toward new innovative materials, including transparent films, reinforcing agents in nanocomposites and paper, biodegradable films, and barriers for packaging and biomedical applications.[11−13]

The successful use of cellulose-based NPs as a stabilizing agent for Pickering emulsion has already been highlighted by several papers,[14−16] and we have previously investigated

Received: February 21, 2014
Accepted: May 14, 2014
Published: May 28, 2014

   dx.doi.org/10.1021/am501077e | *ACS Appl. Mater. Interfaces* 2014, 6, 8263−8273

miniemulsion polymerization in the presence of cellulose nanocrystals.[17]

Starch nanocrystals can be expected to be good candidates for stabilizing Pickering emulsions because of their platelet-sized shape. In addition, the emulsion-stabilizing starch nanoplatelets will result in the formation of nanocomposites upon drying with an expected improved homogeneity when compared to blending of polymers with nanoparticles. This improved dispersion should be beneficial for their reinforcing and barrier effects. The combination of Pickering stabilization using starch platelets with emulsion polymerization should thus result in a one-pot synthesis of a formulation, which will form well-dispersed nanocomposites upon drying. Aside from improved homogeneity in the final composite, in situ Pickering polymerization will also provide several other advantages including a shorter formulation cycle, the removal of the necessary dilution step after mixing of the nanoparticle dispersion and polymer emulsion, and the reduction in quantity of/or omission of the use of organic emulsifying agents. In addition, this strategy is expected to impart a better attachment of the starch nanoplatelets onto the polymer particles, which allows improved tailoring of the nanocomposite characteristics on the nanoscale level, favors nanoparticle individualization,[20] and may even promote formation of chemical linkages between polymer and reinforcement if the appropriate reactive functional groups are present. This in turn is expected to lead to a higher film transparency,[21] a higher nanoparticle reinforcing potential and, for platelet-like particles, improved barrier properties. The use of water as a dispersion medium also has environmental benefits and gives a direct one-pot route to ecofriendly waterborne film-forming nanocomposite dispersions ready for use as water-based coatings and adhesives.

The use of polysaccharide particles or nanoparticles, such as cellulose nanofibrils,[14] cellulose nanocrystals,[15] starch,[22] and recently starch nanocrystals (SNCs)[23] as solid emulsifiers is receiving increasing attention in a broad field of applications such as food technology, cosmetic formulation, and pharmaceutical products. The wide availability of these particles and their relatively ease of production combined with their biodegradability and nontoxic character are all factors that drive forward the use of this sustainable class of nanoparticles as stabilizers to replace synthetic surfactants. However, no work has yet reported the use of SNCs as a solid stabilizer to produce polymer latex dispersions via emulsion polymerization.

In our previous work, the potential of SNCs to stabilize emulsion droplets during miniemulsion polymerization of butyl methacrylate was investigated.[18] We were able to show that while starch nanoplatelets were not sufficient to stabilize the monomer droplets by themselves, they did provide a synergistic stabilization effect when used together with a cationic surfactant, reducing the required surfactant amount by a factor of 4.

This synergistic effect between cationic surfactant and negatively charged nanoparticles has also been seen for TiO_2 and gold nanoparticles.[19] In the present work, we further pursue this approach toward easier and more sustainable processing to enable the use of SNCs as the sole solid stabilizers for polymer latex preparation via emulsion polymerization. This approach brings several advantages compared to our previously published method: (i) the high shear emulsification step, via ultrasonication, required to generate the emulsion droplets, can be omitted, (ii) the use of surfactant can be completely excluded during the polymerization process, (iii) a water-soluble initiator instead of an oil-soluble initiator is used, and (iv) a semicontinuous polymerization process can be envisaged. All of these improvements make this process more sustainable but also contribute to make it easier to be scaled up to an industrial level.

EXPERIMENTAL SECTION

Materials. Butyl methacrylate (BMA, Aldrich, 99 wt %) was distilled under vacuum and kept refrigerated until use. Potassium persulfate (KPS), ascorbic acid (AsA) and H_2O_2 (30%), poly(poly-(ethylene glycol)) methacrylate (Mn = 375) (MPEG), and sodium dioctylsulfano succinate were supplied by Aldrich and used without further purification. Distilled water was used for all the polymerization and treatment processes.

Starch Nanocrystal Preparation. *Sulfuric Acid Hydrolysis.* Sulfuric acid-hydrolysed starch nanocrystals were prepared from waxy maize starch as described elsewhere in detail.[24,25] In short, waxy maize starch was acid hydrolysed for 5 days at 40 °C in a 3.16 M aqueous H_2SO_4 solution while stirring constantly. Complete hydrolysis was confirmed by transmission electron microscopy and by agreement of the final product yield with earlier results. After the hydrolysis, the nanocrystals were separated from the acid by centrifugation at 10,000 rpm at 10 °C. Subsequent washing and centrifugation with distilled water was performed until neutrality of the eluent. A homogeneous dispersion of starch nanocrystals was obtained by using an Ultra Turrax T25 homogenizer for 3 min at 13,500 rpm.

Hydrochloric Acid Hydrolysis. Starch nanoplatelets obtained through hydrochloric acid hydrolysis of waxy maize starch were prepared using the procedure by Putaux et al.[26] Waxy maize starch was mixed with 2M HCl and kept at room temperature for a period of 14 days under sporadic stirring. After 14 days, the nanocrystals were separated from the acid by centrifugation at 10,000 rpm at 10 °C. Subsequent washing and centrifugation with distilled water was performed until neutrality of the eluent. A dilute starch nanocrystal–water mixture was then prepared using an Ultra Turrax T25 homogenizer for 3 min at 13,500 rpm.

Both starch nanoplatelet dispersions were freeze-dried for ease of transport and storage. However, this is not a required step for use in our emulsion preparation. Freeze-drying was performed from a very dilute dispersion. This has been found in our group to reduce aggregation and allow for redispersion.

To distinguish between the two types of SNCs, the subscript H2SO4 and HCl was added to the respective SNC. The physical characteristics of the SNCs used in the present work are given in Table 1.

Table 1. Physical Features of the SNCs Used in the Present Work

SNC	particle size (nm)	ζ-potential (mV)	shape
SNC_{H2SO4}	58	−32	platelet
SNC_{HCl}	51	−2	platelet

The particle size of SNCs from H_2SO_4 and HCl hydrolysis, determined from DLS measurements, was 58 and 51 nm, respectively, and their respective ζ-potentials were −32 and −2 mV.

Emulsion Polymerization. The typical formulation used for the emulsion polymerization in the presence of SNCs is the following: water (30 g), monomers (MBA, 3g), KPS (0.12 g), and SNCs (from 0.06 up to 0.3 g, equivalent to 2−10% of the monomer content).

The following procedure was adopted to implement the emulsion polymerization reaction: the desired amount of starch nanocrystals (SNCs) was weighed and dispersed in 30 mL of water by sonication for 2 min at 70% amplitude (Sonics Vibracel Model CV33) with a 10 s wait each minute. Thereafter, the monomer BMA and initiator were added and emulsified by stirring using a magnetic stir bar for several minutes to create the monomer emulsion. Then, the resulting emulsion was flushed with N_2 and the polymerization was started by

Table 2. Preliminary Results for the Emulsion Polymerization of BMA in the Presence of SNCs as a Sole Stabilizer and Persulfate as an Initiator[a]

	experimental run								
component	1	2	3	4	5	6	7	8	9
water	30	30	30	30	30	30	30	30	30
BMA	5	3	3	3	3	3	3	3	3
MPEG	0	0	0	0	0.03	0.03	0.03	0.03	0.03
KPS	0.1	0.1	0.1	0.1	0.1	0.1	0.1	0.1	0.1
[KCl]	0	0	10^{-2}	0	0	0	0	0	0
SNC_{H2SO4}	8	8	8	10	2	4	6	8	10
aspect	unstable	unstable	unstable	unstable	stable	stable	stable	stable	stable
particle size (nm)					825	642	469	385	342

[a]SNCs prepared via H_2SO_4 hydrolysis; amount in grams.

heating the emulsion to 70 °C. The polymerization is achieved within 3 h.

Polymer Particle Size Determination. The diameters of the polymer particles in the emulsion were measured at 25 °C using a Malvern Nano-Zetasizer ZS Instrument at a fixed scattering angle of 173°. The dispersion was diluted to about 5 wt % with distilled water before starting the measurements. The cumulative average determined from the dynamic light scattering (DLS) correlation curve was fitted with a single exponential decay to determine the polymer particle size distribution. Each measurement was performed in triplicate and the obtained values averaged to obtain the mean polymer particle size.

ζ-Potential Measurement. The ζ-potentials were measured at 25 °C using a laser Doppler electrophoresis apparatus (Malvern Nano-Zetasizer ZS, U.K.). The sample consistency in water was set to 0.01% (w/v). The measurements were performed three times for each sample.

Surface Tension Measurements of Surface Tension. The surface tension was measured using a Prozessor Tensiometer K12 (Krüss, Germany) equipped with a Pt−Ir ring. Measurements were performed using the pull mode. Results are mean values of five repetitive measurements.

Determination of the Surface Coverage of the Dispersion Droplets by SNCs. If we assume the following: (1) the SNCs exhibit a parallepiped shape with average dimensions of 20 × 30 × 4 nm (consistent with TEM results and previous work[25,26]), (2) the emulsion droplets (polymer particles) are monodisperse and spherical, (3) the SNCs lie flat on the surface of the dispersed polymer particles, and (4) all the SNCs are attached to the polymer particle in a monolayer, we can calculate the surface coverage of the dispersion droplets with SNCs using the following approach:

The interfacial area of one monomer droplet/polymer latex particle equals

$$s_p = \pi D_p^2 \tag{1}$$

The effective area covered by one SNC is given by

$$s_{SNC} = ab \tag{2}$$

where a and b are the dimensions of the SNC cross section (20 and 30 nm, respectively)

The total number of monomer or polymer particles can be expressed as

$$N_p = \frac{6m_p}{\rho_p \pi D_p^3} \tag{3}$$

where the total number of SNC particles can be expressed as

$$N_{SNC} = \frac{m_{SNC}}{\rho_{SNC} abh} \tag{4}$$

The interfacial area occupied by the polymer latex (S_p) and the SNCs (S_{SNC}) might be expressed as

$$S_p = N_p \pi D_p^2 = \frac{6m_p}{D_p \rho_p} \tag{5}$$

$$S_{SNC} = N_{SNC} ab = \frac{m_{SNC}}{h\rho_{SNC}} \tag{6}$$

When we assume that the solid SNCs cover a fraction of the polymer particles, then the following relationship holds: $S_{SNC} = C_c S_p$, which gives the following relation between the polymer particle and SNC-covered fraction of the surface area:

$$D_p = 6C_c \left(\frac{m_p}{m_{SNC}}\right)\left(\frac{\rho_{SNC}}{\rho_p}\right)h \tag{7}$$

The surface coverage, C_c, is defined as the ratio of the theoretical maximum surface that can be covered by available SNC particles S_{SNC} and the total surface of polymer particles S_p:

$$C_c = \frac{S_{SNP}}{S_p} \tag{8}$$

$$C_c = \frac{1}{6}\left(\frac{m_{SNC}}{m_p}\right)\left(\frac{\rho_p}{\rho_{SNC}}\right)\left(\frac{D_p}{h}\right) \tag{9}$$

in which ρ_s is the density of SNCs, and h is the thickness of the SNC.

Scanning Electron Microscopy (SEM). Stable emulsions of poly(butyl methacrylate) were quench-frozen in liquid nitrogen and freeze-dried. The freeze-dried powder was deposited on a SEM stud with carbon tape and covered with a thin platinum layer by sputter deposition. The samples were then looked at using an FEI Quanta200 3D DualBeam FIB/SEM operating at a 10−15 kV acceleration voltage.

Nanocomposite Film Preparation. The nanocomposite films were prepared via casting of the nanocomposite dispersion (for the in situ approach) or a mixture of polymer dispersion with an SNC suspension (ex situ approach) in a Teflon mold and stored at 40 °C until water evaporation was completed. A stable polymer dispersion for the ex situ approach was prepared via a standard emulsion polymerization as follows: BMA was polymerized via emulsion polymerization in the presence of sodium dioctylsulfano succinate (3% with respect to monomer content) as an anionic surfactant and MPEG (3% based on BMA) to bring about stability during the emulsion polymerization.

A transparent to translucent film, depending on the nanofiller content and the mode of dispersion preparation, was obtained with a thickness of 200−300 μm.

RESULT AND DISCUSSION

To probe the stabilization behavior of SNC_{H2SO4} during BMA emulsion polymerization, a series of experiments under different conditions such as the SNC content, comonomer, and ionic strength were performed (Table 2). The polymer-

dx.doi.org/10.1021/am501077e | ACS Appl. Mater. Interfaces 2014, 6, 8263−8273

ization reaction was carried out in batch mode by simply adding the desired amount of monomer to the suspension containing the desired amount of SNC_{H2SO4} and initiator. The terms "stable" and "unstable" dispersion were used to distinguish between the formation of a stable polymer latex after emulsion polymerization ("stable") or the formation of coarse polymer lumps visible to the naked eye resulting from agglomeration of polymer particles during polymerization ("unstable").

From these experiments, the following conclusions could be drawn: (1) the polymerization reaction without MPEG comonomer was found to be too slow and the dispersion proved to be unstable, resulting in the formation of coarse lumps of polymer particles swollen with monomer after several hours at 70 °C. Increasing the starch content up to 10 wt % was unsuccessful in improving the monomer conversion and no stable polymer dispersion was formed even after 8 h of reaction at 70 °C. It is likely that the hydrophilic character of SNC_{H2SO4} along with their negatively charged surface prevented the efficient attachment of the SNC onto the nucleated polymer particles, in agreement with our previous work.[18] (2) The addition of KCl up to 10^{-2} M was ineffective in improving the stability of the dispersion during polymerization. Adding KCl compresses the charged double layer so that a slight instability of the solid nanoparticles in the aqueous environment is introduced. This is expected to force them to accumulate on the monomer droplet surface. In Pickering emulsions, the addition of monovalent electrolyte is often reported to enhance the emulsion stability,[27] but it did not prove effective here. (3) The addition of 10% isopropyl alcohol, known to increase the monomer solubility in water and accordingly to accelerate the polymerization rate, did not improve the dispersion stability. (4) With the addition of MPEG auxiliary monomer at a level of 3 wt % of total monomer content, stable polymer dispersions free of any coagulum where formed. The dispersion further exhibited a monomodal distribution, even when the content of SNC_{H2SO4} was only 2% based on the monomer content. As the SNC content increased, the polymer particle size decreased. The same polymerization carried out without SNC_{H2SO4} did not lead to a stable dispersion in any polymerization. The SNC_{H2SO4} thus contributes considerably to colloidal stability in the presence of the MPEG comonomer.

MPEG comonomer is thus essential in achieving successful emulsion polymerization of BMA in the presence of SNC_{H2SO4} and this without a surfactant. We presume that in the presence of the MPEG comonomer, the wettability of SNC_{H2SO4} was modified to make them more likely to adsorb onto the surface of the monomer droplet/nucleated polymer particles. It is likely that the presence of the short chain poly(ethylene glycol) in the comonomer favors adsorption of MPEG onto SNC_{H2SO4}. The poly(ethylene glycol) polymer has previously been shown to absorb well onto SNC surfaces.[24,28] Once the particle is nucleated, the terminal double bond of the MPEG will be involved in the polymerization reaction and accordingly will promote the irreversible anchoring of the SNC onto the polymer particles. It is worth noting that no stable emulsion is formed when the monomer is added to the SNC_{H2SO4} suspension, even in the presence of MPEG, meaning that the SNCs were not able to stabilize the monomer droplets in water. This is likely the consequence of the preferential adsorption of SNC_{H2SO4} onto the small nucleated polymer particles rather than the larger monomer droplet.

By increasing the content of SNC_{H2SO4}, a continuous decrease in the polymer particle size can be seen over the whole range of SNC contents (Figure 1). This is both evident for sulfuric acid and hydrochloric acid derived SNCs, even

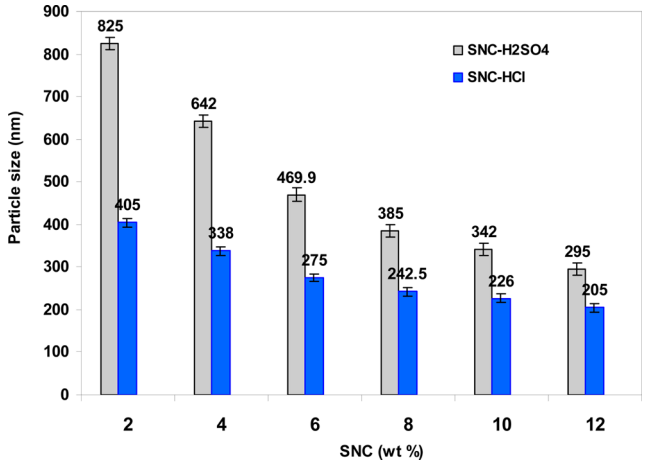

Figure 1. Evolution of the polymer particle size as a function of SNC content (solid content = 10%, SNC from H_2SO_4 and HCl hydrolysis, initiator KPS).

though the trend is much more pronounced for H_2SO_4-hydrolysed SNCs. This can be expected as sulfuric acid exposure will result in the grafting of a small amount of sulfate half-esters on the SNC surface, giving increased stabilization of the SNCs in water due to electrostatic repulsion. This repulsion will be transferred onto the polymer droplets upon adsorption of the SNCs onto their surface. The strong dependence of the particle size with SNC content further emphasizes the key role of SNCs onto the stabilization process. Actually, in Pickering stabilization, the particle size of the dispersed phase is directly correlated with the amount of the solid particles. Assuming the following hypothesis, (i) the SNC being monodisperse platelets with close packing geometry, (ii) polymer particles being monodisperse spherical particles, and (iii) SNC being fully adsorbed at the polymer−water interface with no excess particles in the water phases over the full concentration range, then the relation between the mean particle size and the SNC content of SNC might be expressed by eq 3.

Furthermore, if we assume that full coverage is not necessary to ensure colloidal stabilization, then the relationship between the polymer droplet diameter and SNC content is expressed by eq 7 and

$$\frac{1}{D_p} = \frac{1}{6C_c h}\left(\frac{\rho_p}{\rho_{SNC}}\right)\left(\frac{m_{SNP}}{m_p}\right) = \left(\frac{\rho_p}{6C_c h \rho_{SNC} m_p}\right) m_{SNP} \quad (10)$$

The polymer particle diameter should thus be inversely proportional with the SNC content as long as the emulsion stability is driven by Pickering stabilization. As shown in Figure 2, a linear evolution of the inverse diameter of the polymer particles ($1/D$) vs SNC is indeed observed over the whole range of compositions, confirming that the interfacial area was truly proportional to the SNC content and the polymer latex dispersion was generated by Pickering emulsion polymerization.

When we look to the ζ-potential evolution of the polymer particles vs SNC content (Figure 3), we can note that the absolute value of the ζ-potential is higher than that of the pristine SNCs (around −32 mV) when their content is lower than 8%, meaning that the surface charge density of the

dx.doi.org/10.1021/am501077e | ACS Appl. Mater. Interfaces 2014, 6, 8263−8273

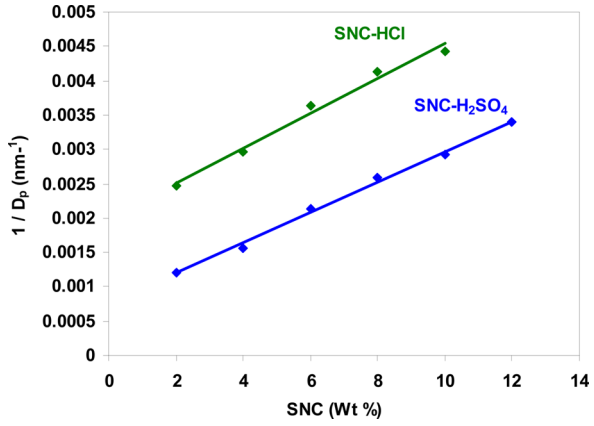

Figure 2. Inverse diameter of the polymer particles ($1/D_p$) vs SNC content during the Pickering emulsion polymerization in the presence of SNCs extracted through H_2SO_4 and HCl hydrolysis.

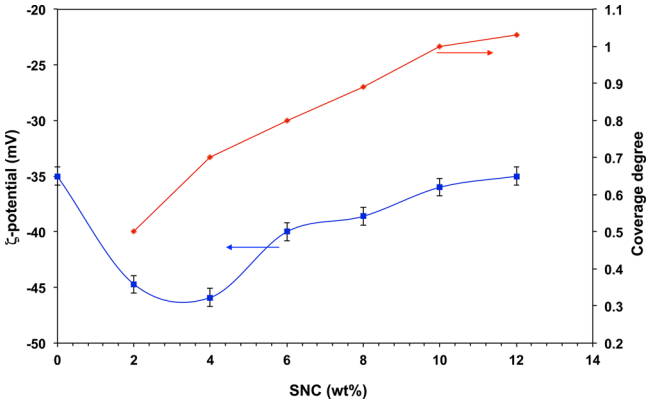

Figure 3. Evolution of the degree of coverage and ζ-potential as a function of SNC content during Pickering emulsion polymerization of BMA in the presence of SNCs extracted through H_2SO_4 hydrolysis.

polymer particles exceeds that of the SNCs in this domain. Comparing these data with the SNC coverage fractions of the polymer particles, we note that in the range of 2−6% SNC, the degree of coverage is below 1. Therefore, the higher ζ-potential in this domain is indicative that more surface charge was present on the polymer particles than the surface charge supplied by the adsorbed SNC_{H2SO4}. Given the fact that KPS decomposition generates SO_4^{-} radicals that will initiate the polymerization in the aqueous phase, we presume that the uncovered part of the polymer particles held negative charges stemming from the initiator residue. The presence of these negative charges is likely to contribute to the stabilization process as the SNC_{H2SO4} content is lower than 8%.

To confirm this hypothesis, emulsion polymerization was carried out in the presence of 8% SNC_{H2SO4} with different initial concentrations of KPS. Results collected in Table 3 show

Table 3. Effect of Initiator Amount (KPS) on the Particle Size (in nm) during the Pickering Emulsion Polymerization of BMA in the Presence of 8% SNPs[a]

initiator (%[b])	2	4	6	8
SNC_{H2SO4}	410	385	358	254
SNC_{HCl}	284	242	220	

[a]SNC subscript denotes acid used for extraction. [b]Based on the monomer content.

a decrease in the particle size with increasing KPS amount. Increasing the KPS content from 2% up to 4% led to decrease of the particle size from 410 to 254 nm. This significant reduction in particle size is an indication of the contribution by the sulfate moiety to the stabilization process, presumably through the accumulation of the terminal SO_4^{-} groups at the polymer tails in the outer layer of the polymer particles.

To investigate the effect of the SNC surface charge on their stabilization ability, a set of emulsion polymerizations was carried out using SNCs prepared via HCl hydrolysis. The SNCs prepared via HCl hydrolysis (SNC_{HCl}) exhibited a lower surface charge density, as attested by their lower ζ-potential compared to the SNCs extracted through H_2SO_4 hydrolysis (−2 mV for the former compared to −32 mV for the latter). Adopting the same polymerization conditions, in terms of initiator amount, temperature, and comonomer content, it can be seen (Figure 1) that a lower polymer particle size was systematically obtained when the polymerization was carried out with SNC_{HCl}. Furthermore, the addition of the auxiliary monomer MPEG was not necessary to improve latex stability. Stable dispersions were obtained in the absence of MPEG with a lower particle size when SNC_{HCl} were used. It is likely that the higher surface charge density of SNC_{H2SO4} enhanced their stability in the aqueous phase, and accordingly, reduced their aptitude to adsorb at the polymer/water interface. In addition, a similar trend in the dependence of the particle size vs solids content of the nanoparticles is seen, with a linear evolution of the inverse diameter of the polymer particles ($1/D_p$) vs SNC over the whole range of composition (Figure 2). This confirms again that the polymer latex dispersion was truly obtained via Pickering emulsion polymerization.

An additional reason to account for the higher particle size when the emulsion polymerization is carried out with SNC_{H2SO4} using KPS as an initiator is the electrostatic repulsion between the SNCs' surface charge and the negative charge of the KPS residue at the end of the polymer chains. This repulsion might act against the adsorption of the SNC_{H2SO4} on the nucleated polymer particles. To verify whether this effect is important, KPS was replaced with H_2O_2/ascorbic acid as the initiator, the decomposition of which does not generate ionic initiator radicals, and the emulsion polymerization was performed under the same conditions as for KPS. As shown in Figure 4, a significantly lower particle size

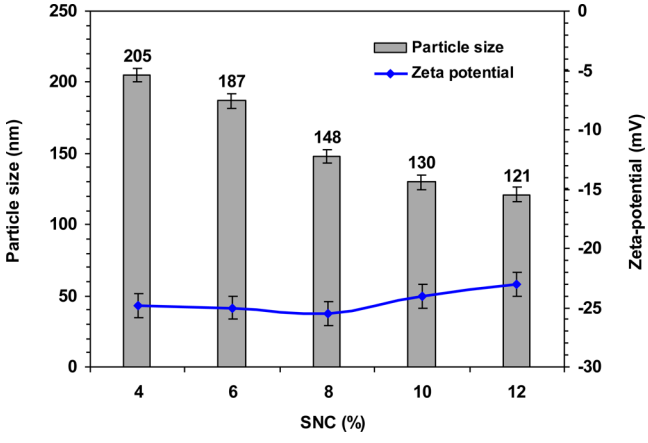

Figure 4. Evolution of the polymer particle size and ζ-potential as a function of SNC content using H_2O_2 as the initiator: solid content = 10%, SNCs from H_2SO_4 hydrolysis, initiator H_2O_2/ascorbic acid.

dx.doi.org/10.1021/am501077e | ACS Appl. Mater. Interfaces 2014, 6, 8263−8273

Table 4. Particle Size, ζ-Potential, and Surface Tension of the Latex Dispersion Prepared via Pickering Emulsion Polymerization in the Presence of 8% SNCs and KPS or H_2O_2 as the Initiator[a]

initiator%MPEG	KPS-3%MPEG		KPS-0%MPEG		H_2O_2-3%MPEG[a]		H_2O_2-0%MPEG	
type of SNC	H_2SO_4	HCl	H_2SO_4	HCl	H_2SO_4	HCl	H_2SO_4	HCl
particle size (nm)	385	253		242	148	144	143	140
ζ-potential (mV)	−37	−11		−8	−22	−3	−24	−3
γ (mN/m)	52	41		63	56	51	64	65

[a]No formation of a stable emulsion for KPS initiation, 0% MPEG and SNC_{H2SO4}.

was obtained for the H_2O_2/ascorbic acid initiator system, irrespective of the SNC_{H2SO4} content. For instance, at 8% SNC_{H2SO4}, the polymer particle size decreased from 350 nm to about 145 nm when KPS was replaced with H_2O_2/ascorbic acid. The same trend was noted for a 6 and 10% SNC_{H2SO4} content. Furthermore, using the noncharged initiator, the addition of auxiliary monomer MPEG is no longer necessary for a stable dispersion during polymerization, given that its presence does not affect the final particle size of the polymer dispersion.

One might ask if the presence of MPEG is likely to impart the required interfacial tension reduction that explains the stabilization effect. To investigate this issue, surface tension and ζ-potential measurements were carried out on latex dispersions prepared via Pickering emulsion polymerization in the presence of 8% SNCs with and without MPEG and using either KPS or H_2O_2 initiators (Table 4). Two main conclusions could be drawn; the first one is that MPEG enhanced the colloidal stability only in the presence of the charged SNC_{H2SO4} and when KPS was used as the initiator. With H_2O_2 initiation, no obvious difference in the particle size was observed with or without MPEG use for both SNC_{H2SO4} and SNC_{HCl}, even though SNC_{H2SO4} led to a higher absolute value of ζ-potential. Secondly, the surface tension was seen to decrease when MPEG was used as a comonomer. Still, the attained values are not as low as those observed before the start of the polymerization reaction and the addition of SNCs (i.e, 34 mN/m). The low surface tension prior to polymerization is likely the result of accumulation of the PEG ends of MPEG at the monomer droplet surface. The slight decrease in the surface tension seen after polymerization in the presence of MPEG (Table 4) can be explained by the adsorption of MPEG onto the SNC surface and to their copolymerization with BMA.

This is also supported by the absence of any significant surface tension change before and after emulsion polymerization in the presence of SNCs but in the absence of MPEG. This further demonstrates that interfacial tension reduction is not the operative stabilization mechanism in this emulsion polymerization, leaving SNC adsorption during the polymer nucleation step as the driving force for the stabilization process (i.e., Pickering emulsion stabilization). Indeed, generally, the presence of the particles was shown not to affect the interfacial tension and surface tension.[29]

Furthermore, because no stable emulsion polymerization could take place in the absence of SNCs, even in the presence of MPEG, it is reasonable to assume that the success of the emulsion polymerization with the formation of polymer particles with a size between 150 to 250 nm is brought about by Pickering stabilization with SNCs. This hypothesis is further supported by the steady decrease in the particle size as the content of SNCs is going up.

The evolution of the apparent polymer particle size during the emulsion polymerization was monitored by dynamic light scattering (DLS), as shown in Figure 5. As the polymerization proceeded, the polymer particle size increased continuously

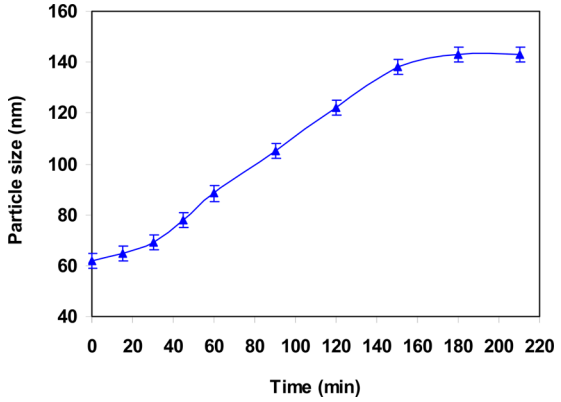

Figure 5. Evolution of the polymer particle size vs time during the course of the Pickering emulsion polymerization in the presence of 8% SNC, using H_2O_2−ascorbic acid as the initiator.

until depletion of the monomer droplet and the dissolved monomer. Moreover, it can be seen also that the polymerization reaction is completed within 3 h, which is an acceptable time period with regard to the emulsion or radical polymerization.

Based on the above data, the mechanism by which Pickering emulsion polymerization of BMA takes place in the presence of SNCs might be proposed to follow an homogeneous nucleation process: upon initiator addition, monomers dissolved in the aqueous phase react with decomposed initiators. They then form oligomers until reaching a critical length to precipitate, giving rise to nucleated polymer particles. These primary polymer particles are then stabilized by SNCs that were previously either adsorbed onto monomer droplets or by free SNCs from the aqueous phase, and will grow by diffusion of monomer from the monomer droplets to the nucleated polymer particle. As the polymer particles grow, their interfacial area increases and additional solid SNCs are needed to ensure stabilization and avoid particle aggregation. These are supplied by the direct adsorption of SNCs on the growing polymer particle or resulted from the aggregation of the nucleated polymer particles until reaching an optimum surface coverage. The higher interfacial energy of the polymer particles compared to the interfacial energy of the monomer droplets[30] might be the reason for the higher adhesion aptitude of SNCs onto polymer particles during the homogeneous nucleation process. This would account for the excellent stabilization of the polymer particles compared to the stabilization of the monomer droplets. A schematic illustration of this process is shown in Scheme 1.

Mechanical Properties. One of the main goals of incorporating nanofillers within a polymer matrix is the

Scheme 1. Schematic Illustration of the Processes Involved in the in Situ Emulsion Polymerization of SNC-based Nanocomposite Dispersion

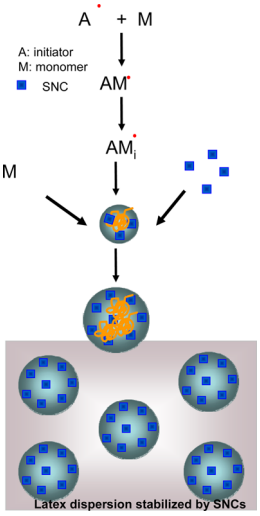

improvement of the mechanical properties at a low filler loading. However, the processing route for composite materials significantly affects the reinforcing potential of the (nano)filler as it dictates the extent of homogeneity and individualization of the filler material. Given the high surface area of nanofillers and their strong tendency to self-associate, the properties of polymer nanocomposites are especially strongly dependent on the effectiveness of the dispersion of the nanofiller, in addition to their fractal clustering within the polymer matrix and their interfacial interaction with the polymer. This is particularly the case for polysaccharide based nanoparticles, where their inherent polarity and hydrogen-bonding tendency complicates homogeneous dispersion in a hydrophobic polymer matrix. This explains why the most common route for the processing of polysaccharide nanoparticle composites relies on the mixing of an aqueous suspension of polysaccharide NPs with a waterborne polymer, followed by solvent casting and water evaporation. Evidently, this approach is time-consuming and limits their commercial application, despite their well-recognized exceptional reinforcing potential.[9,13]

It is thus important to investigate whether the in situ emulsion polymerization route might affect the reinforcing potential of SNCs. The temperature dependence of the storage tensile modulus, E', as a function of temperature at 1 Hz for solvent-cast nanocomposite films from the in situ and the ex situ prepared samples with different SNC contents are shown in Figure 6. Two behaviors are observed; below the glass transition temperature, no significant variation in the storage modulus is detected upon the incorporation of SNC. On the other hand, above the glass transition, the storage modulus is more sensitive to the presence of the nanofiller and increased significantly with SNC addition, in line with the well-known reinforcing effect of nanobased polysaccharide nanoparticles.[31] This means that SNCs are most effective in restricting the mobility of the polymers chains above Tg.

To further highlight the stiffening effect imparted by the addition of SNCs the evolution of the relative modulus $E_r = E_N/E_{mat}$ (with E_N and E_{mat} as the storage modulus of the nanocomposite and unfilled matrix, respectively, measured in the rubbery region taken here at 70 °C) versus the SNC content was drawn for the nanocomposite films prepared via Pickering emulsion polymerization and via ex situ mixing (Figure 7). In both processing routes, the presence of SNCs in the polymer matrix led to a continuous rise in the relative modulus, clearly confirming the reinforcing potential of the

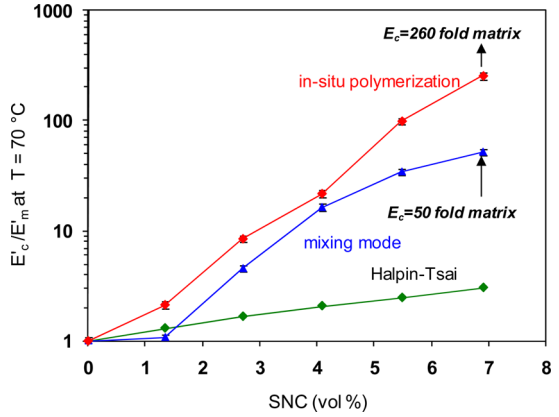

Figure 7. Evolution of the relative storage modulus versus SNC content at 70 °C for nanocomposite films prepared either via in-situ emulsion polymerization , and ex situ mixing using SNCs prepared via H_2SO_4 hydrolysis.

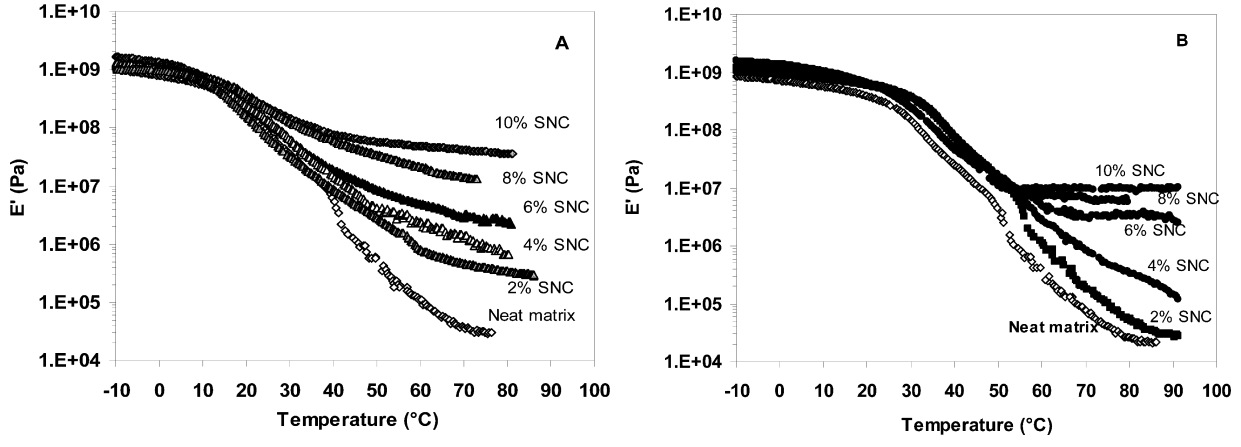

Figure 6. Evolution of the storage tensile modulus, E', versus temperature at 1 Hz for nanocomposites obtained from (A) in situ polymerization and (B) ex situ polymerization followed by mixing with an SNC dispersion using SNC_{H2SO4}.

dx.doi.org/10.1021/am501077e | ACS Appl. Mater. Interfaces 2014, 6, 8263−8273

SNCs. However, above 6 wt % SNC, the magnitude of the reinforcing effect diverged considerably for the samples prepared via in situ polymerization. For instance, at 8 and 10 wt % (corresponding to 5.48 and 6.9 vol %) SNCs, the modulus is respectively about 100 and 250 times higher than the modules of the neat matrix when Pickering emulsion polymerization was adopted, while the increase is only 34 and 50 times with respect to the neat matrix modulus when ex situ mixing was used to prepare the nanocomposite film. Referring to the literature, such a huge reinforcement coming from SNCs is the highest ever reported for SNC-based nanocomposite films.[31] To better understand the origin of the superior reinforcing efficiency observed in SNC-based nanocomposites, the Halpin−Tsai model[32] was used to see if the experimental data could be fitted with this model. This model is a semi-empirical model initially developed to predict the stiffness of unidirectional composites as a function of reinforcement aspect ratio, and then was extended to nanocomposite materials.[33] It has been successfully used to predict the modulus of clay nanocomposites.[34] According to the Halpin−Tsai model, the longitudinal and transverse modulus can be calculated as

$$\frac{E_c}{E_m} = \frac{1 + \zeta\eta\varphi}{1 - \eta\varphi} \tag{11}$$

where E_c and E_m stand for the Young's modulus of the composite and the matrix, respectively, ζ is a shape factor dependent upon filler geometry and loading direction, φ is the volume fraction of filler and η is given by

$$\eta = \frac{E_f/E_m - 1}{E_f/E_m + \zeta} \tag{12}$$

with $\zeta = 2L/D$ for the modulus in the longitudinal direction, and $\zeta = 2$ for the modulus in the transverse direction.

For a lamellar shape filler, eqs 11 and 12 may still be used by replacing (L/D) with (D/h), where D and h are, respectively, the diameter and thickness of the platelets.

If the longitudinal modulus E_L and the transverse modulus E_T are known, then the effective modulus of the composite with randomly oriented fibers and platelets in all three orthogonal directions is given by

$$E_{3D}^{platelet} = 0.49E_L + 0.51E_T \tag{13}$$

Adopting the following parameters for SNC: L = 30 nm, h = 5 nm, E_f = 20 GPa, results shown in Figure 7 reveal that the Halpin−Tsai model failed to fit the experimental data. The increment in the modulus of the nanocomposite is much higher than that estimated based on the Halpin−Tsai model, for SNC contents exceeding 1.5 vol %. If we consider that this mean-field model assumes no interactions between fillers, then the analysis of the mechanical behavior of SNC-based composites needs to take into account the topological arrangement of the fillers and their likely interactions. Actually, the high specific surface of SNC, their low thickness, and their numerous surface hydroxyl groups will lead to filler/filler interactions driven by hydrogen bonding, giving rise to the formation of a fillers network within the host matrix. The resulting network may be the reason for the unusually high reinforcing effect of the SNCs in nanocomposites prepared through the in-situ polymerization approach. This mechanism was demonstrated to be responsible for the excellent reinforcement in cellulose nanocrystal reinforced nanocomposites.[35]

The higher reinforcing potential of SNCs when the nanocomposite was prepared via in situ polymerization was also highlighted in our previous work when the nanocomposite dispersion was prepared via a minemulsion route and in the presence of a cationic surfactant.[18] However, in the present case, the effect is more pronounced and a simple emulsion polymerization approach without any added surfactant was implemented. To explain this unusual reinforcing effect, three reasons are proposed: (i) the emulsion polymerization route ensured efficient individualization and uniform dispersion of the SNC within the polymer matrix, (ii) the anchoring of the SNC upon the particle surface enhances the interaction between the nanofiller and the host matrix thus favoring the transfer of the stress to the rigid nanofiller, and (iii) the possible filler−filler interactions potentially leading to a percolated network should also be taken into consideration.

It is worth noting that the huge reinforcing effect observed for films prepared via the in situ emulsion polymerization route is quite similar irrespective of whether SNCs from H_2SO_4 or HCl hydrolysis were used. This further supports that the huge reinforcing effects imparted by SNCs is due to the use of the in situ route adopted for the emulsion preparation.

Optical Properties. In addition to the mechanical reinforcing effect provided by the inclusion of nanofillers in a polymer matrix, the optical transparency of the polymeric matrix is another aspect that is often aimed to be preserved. For nanocomposite materials, the reduction in transparency is brought about by light scattering particle by the randomly dispersed particles. In general, 40 nm is the upper limit of the nanoparticle diameter to avoid intensity loss of the transmitted light due to Rayleigh scattering.[36] Given the mismatch in the refractive index (RI) of starch (1.58)[37] and the host matrix (1.48),[38] the critical factor in the transparency of SNC-based nanocomposites is the width of the nanofiller or more specifically the effective cross-sectional area of a scattering and its dispersion level within the host polymer matrix.

The optical transparency of the nanocomposite films with 200−300 μm in thickness were analyzed by transmittance measurements in the visible wavelength range. To avoid the effect of the variation of the film thickness, the film transmittance was normalized to a 200 μm thickness using the Beer−Lambert law. To evaluate the optical transparency of the nanocomposites for different nanoparticle contents, the transmittance at 700 nm was used, and results are shown in Figure 8. It is interesting to note that the degree of transparency increases as the SNC content increases, and at 12% SNC, the film transparency is close to that of the neat matrix. The transmittance of the nanocomposite film was comparable to that of the neat matrix at around 90−95% from 600 to 800 nm, but fell to around 85% at shorter wavelengths. This behavior is unusual in nanocomposite-based materials, where the increase in the nanofiller content inevitably leads to a drop in the transparency as a consequence of the aggregation tendency of the NPs as their content exceeds a critical threshold. This finding suggests an improvement in the dispersion degree of the nanofiller within the polymer matrix with increasing content of the nanofiller, since any clustering would inevitably lead to substantial light scattering and loss of optical clarity. The strong dependence of transmittance on wavelength (lower transmittance at λ < 500 nm) is the consequence of Rayleigh scattering whose intensity is inversely proportional to the fourth power of the wavelength ($I \propto 1/\lambda^4$). If we assume that Rayleigh scattering prevails for particles with

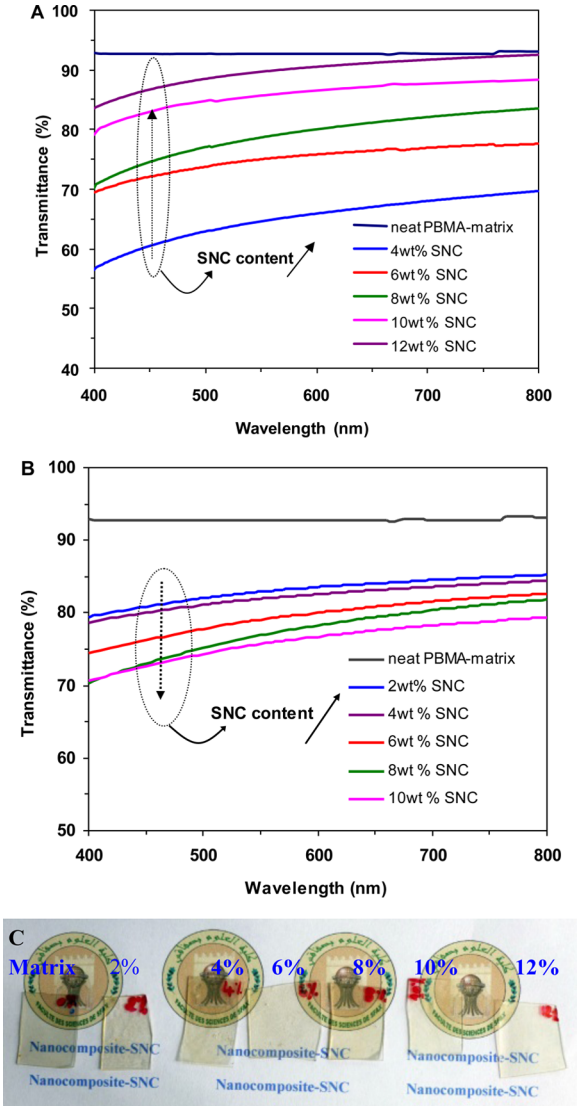

Figure 8. Transmittance spectra recorded in the visible wavelength range (thickness normalized to 200 μm) for nanocomposite film prepared via (A) the in situ and (B) the ex situ polymerization route. (C) Digital photos of nanocomposite film prepared via the in situ approach.

a square section lower than 40 nm (about $\lambda_{vis}/10$), then such dependence provides further proof of the good dispersion of the SNC within the host matrix.

The improvement in the transparency degree, namely above a 6% nanofiller content, along with the huge enhancement in the reinforcing brought about by the SNCs when the in situ emulsion polymerization route is adopted, constitutes the two key results of the present work. Actually, when the mixing route is used, a decrease in the transparency is noted and the reinforcing effect is quite modest (Figures 7 and 8b).

Morphology of the Polymer Particles. Freeze-dried nanocomposite dispersions prepared via emulsions polymerization in the presence of 8 wt % SNCs from both H_2SO_4 and HCl hydrolysis were visualized by field emission (FE)-SEM (Figure 9). As shown in Figure 9, irrespective of the SNCs type, the polymer particles prepared via emulsion polymerization were homogeneous spheres with a raspberry-like morphology. No free SNCs were visible on the analyzed surface or anywhere else, which might be a confirmation that all of the NPs were attached on the polymer particles. One possible explanation for the raspberry-like surface is based on the mechanistic aspect of the emulsion polymerization in the presence of SNCs (Scheme 1). As previously proposed, once the nucleated particles are formed and their size is increasing, partial aggregation among the nucleated particles stabilized by SNCs might take place to ensure enough surface coverage by the SNC particles. This aggregation behavior may lead to the observed polymer particle surface.

CONCLUSIONS

In summary, a highly efficient route to stable colloidal polymer−SNC nanocomposite particles is reported. This new protocol involves a one-pot aqueous emulsion polymerization at 70 °C using a water-soluble radical initiator and SNCs as the sole stabilizing agent in the absence of any added surfactant or nonaqueous cosolvent. The HCl-hydrolysed starch nanocrystals were found to give better stabilization and smaller polymer particles.

After the film-formation process at room temperature, the nanocomposites formed by drop-casting the polymer Pickering emulsions showed better mechanical properties and optical transparency than could be obtained by blending the polymer emulsion with a nanocrystal dispersion, showing the one-pot route to nanocomposite precursors to be doubly advantageous.

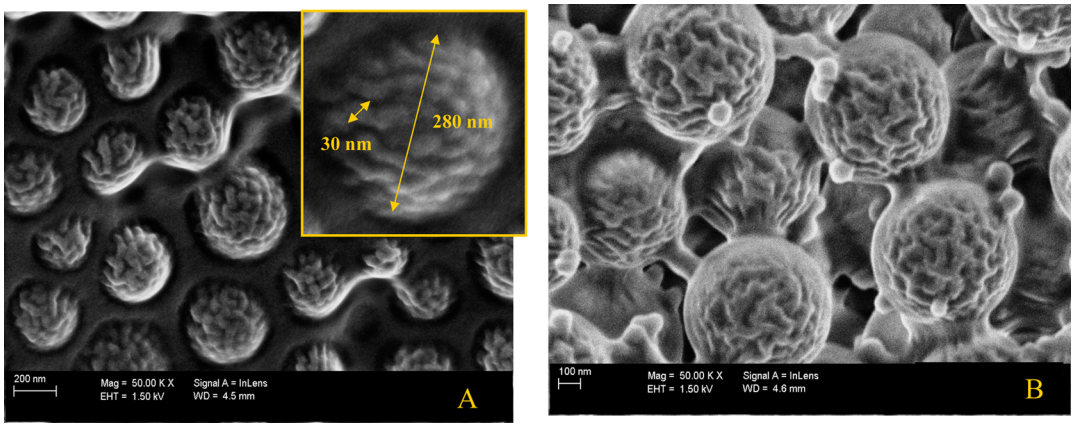

Figure 9. FE-SEM micrographs of freeze-dried poly(butyl methacrylate) dispersions prepared via in situ emulsion polymerization in the presence of 8 wt % SNC (A) prepared via H_2SO_4 and (B) HCl hydrolysis.

dx.doi.org/10.1021/am501077e | ACS Appl. Mater. Interfaces 2014, 6, 8263−8273

Apart from facilitating the usage of the SNCs as a nanofiller, this synthesis approach opens the way toward wide possible potential for the production of highly transparent, mechanically tough nanocomposite films, coating, or adhesives.

AUTHOR INFORMATION

Corresponding Authors

*S. Boufi. E-mail: sami.boufi@fss.rnu.tn.

*W. Thielemans. E-mail: wim.thielemans@kuleuven.be.

Notes

The authors declare no competing financial interest.

ACKNOWLEDGMENTS

This work was financially supported by the "PHC Utique" program of the French Ministry of Foreign Affairs and Ministry of higher education and research and the Tunisian Ministry of higher education and scientific research in the CMCU project number 15G1115

REFERENCES

(1) Chevalier, Y.; Bolzinger, M.-A. Emulsions Stabilized with Solid Nanoparticles: Pickering Emulsions. *Colloids Surf., A* **2013**, *439*, 23−34.

(2) Butler, L. N.; Fellows, C. M.; Gilbert, R. G. Effect of Surfactants used for Binder Synthesis on the Properties of Latex Paints. *Prog. Org. Coat.* **2005**, *53*, 112−118.

(3) Kralchevsky, P. A.; Ivanov, I. B.; Ananthapadmanabhan, K. P.; Lips, A. On the Thermodynamics of Particle Stabilized Emulsions: Curvature Effects and Catastrophic Phase Inversion. *Langmuir* **2005**, *21*, 50−63.

(4) Vignati, E.; Piazza, R.; Lockhart, T. P. Pickering Emulsions: Interfacial Tension, Colloidal Layer Morphology, and Trapped-Particle Motion. *Langmuir* **2003**, *19*, 6650−6656.

(5) Song, X.; Zhao, Y.; Wang, H.; Du, Q. Fabrication of Polymer Microspheres Using Titania as a Photocatalyst and Pickering Stabilizer. *Langmuir* **2009**, *25*, 4443−4449.

(6) Bon, S. A. F.; Chen, T. Pickering Stabilization as a Tool in the Fabrication of Complex Nanopatterned Silica Microcapsules. *Langmuir* **2007**, *23*, 9527−9530.

(7) Teixeira, R. F. A.; McKenzie, H. S.; Boyd, A. A.; Bon, S. A. Pickering Emulsion Polymerization Using Laponite Clay as Stabilizer To Prepare Armored "Soft" Polymer Latexes. *Macromolecules* **2011**, *44*, 7415−7422.

(8) MacDonald, S. M.; Fletcher, P. D. I.; Cui, Z. G.; Opallo, M. C.; Chen, J. Y.; Marken, F. Carbon Nanoparticle Stabilised Liquid-Liquid Micro-Interfaces for Electrochemically Driven Ion-Transfer Processes. *Electrochim. Acta* **2007**, *53*, 1175−1181.

(9) Dufresne, A. *Nanocellulose: From Nature to High Performance Tailored Materials*; Walter de Gruyter GmbH Co.KG: Berlin, 2012.

(10) Kalia, S.; Boufi, S.; Celli, A.; Kango, S. Nanofibrillated Cellulose: Surface Modification and Potential Applications. *Colloid Polym. Sci.* **2014**, *292*, 5−31.

(11) LeCorre, D.; Bras, J.; Dufresne, A. Influence of the Botanic Origin of Starch Nanocrystals on the Morphological and Mechanical Properties of Natural Rubber Nanocomposites. *Macromol. Mater. Eng.* **2012**, *297*, 969−987.

(12) Fukuzumi, H.; Saito, T.; Wata, T.; Kumamoto, Y.; Isogai, A. Transparent and High Gas Barrier Films of Cellulose Nanofibers Prepared by TEMPO-Mediated Oxidation. *Biomacromolecules* **2009**, *10*, 162−165.

(13) LeCorre, D.; Dufresne, A.; Rueff, M.; Khelifi, B.; Bras, J. All Starch Nanocomposite Coating for Barrier Material. *J. Appl. Polym. Sci.* **2014**, *131*, 39826.

(14) Andresen, M.; Stenius, P. Water-in-Oil Emulsions Stabilized by Hydrophobized Microfibrillated Cellulose. *J. Dispersion Sci. Technol.* **2007**, *28*, 837−844.

(15) Kalashnikova, I.; Bizot, H.; Cathala, B.; Capron, I. New Pickering Emulsions Stabilized by Bacterial Cellulose Nanocrystals. *Langmuir* **2011**, *27*, 7471−7479.

(16) Zoppe, J. O.; Venditti, R. A.; Rojas, O. J. Pickering Emulsions Stabilized by Cellulose Nanocrystals Grafted with Thermo-Responsive Polymer Brushes. *J. Colloid Interface Sci.* **2012**, *369*, 202−209.

(17) Ben Elmabrouk, A.; Thielemans, W.; Dufresne, A.; Boufi, S. Preparation of Poly(Styrene-co-Hexylacrylate)/Cellulose Whiskers Nanocomposites via Miniemulsion Polymerization. *J. Appl. Polym. Sci.* **2009**, *114*, 2946−2955.

(18) BelHaaj, S.; Ben Mabrouk, A.; Thielemans, W.; Boufi, S. A One-Step Miniemulsion Polymerization Route towards the Synthesis of Nanocrystal Reinforced Acrylic Nanocomposites. *Soft Matter* **2013**, *9*, 1975−1984.

(19) Kawazoe, A.; Kawaguchi, M. Characterization of Silicone Oil Emulsions Stabilized by TiO_2 Suspensions Pre-Adsorbed SDS. *Colloids Surf., A* **2011**, *392*, 283−287.

(20) Ben Mabrouk, A.; Vilar, M. R.; Magnin, A.; Belgacem, M. N.; Boufi, S. Synthesis and Characterization of Cellulose Whiskers/Polymer Nanocomposite Dispersion by Mini-Emulsion Polymerization. *J. Colloid Interface Sci.* **2011**, *363*, 129−136.

(21) Fielding, L. A.; Tonnar, J.; Armes, S. P. All-Acrylic Film-Forming Colloidal Polymer/Silica Nanocomposite Particles Prepared by Aqueous Emulsion Polymerization. *Langmuir* **2011**, *27*, 11129−11144.

(22) Marku, D.; Wahlgren, M.; Rayner, M. Characterization of Starch Pickering Emulsions for Potential Applications in Topical Formulations. *Int. J. Pharm.* **2012**, *428*, 1−7.

(23) Li, C.; Sun, P.; Yang, C. Emulsion Stabilized by Starch Nanocrystals. *Starch/Staerke* **2012**, *64*, 497−502.

(24) Thielemans, W.; Belgacem, M. N.; Dufresne, A. Starch Nanocrystals with Large Chain Surface Modifications. *Langmuir* **2006**, *22*, 4804−4810.

(25) Angellier, H.; Choisnard, L.; Molina-Boisseau, S.; Ozil, P.; Dufresne, A. Optimization of the Preparation of Aqueous Suspensions of Waxy Maize Starch Nanocrystals Using a Response Surface Methodology. *Biomacromolecules* **2004**, *5*, 1545−1551.

(26) Putaux, J.-L.; Molina-Boisseau, S.; Momaur, T.; Dufresne, A. Platelet Nanocrystals Resulting from the Disruption of Waxy Maize Starch Granules by Acid Hydrolysis. *Biomacromolecules* **2003**, *4*, 1198−1202.

(27) Yang, F.; Liu, S.; Xu, J.; Lan, Q.; Wei, F.; Sun, D. Pickering Emulsions Stabilized Solely by Layered Double Hydroxide Particles: The Effect of Salt on Emulsion Formation and Stability. *J. Colloid Interface Sci.* **2006**, *302*, 159−169.

(28) Labet, M.; Thielemans, W.; Dufresne, A. Polymer Grafting onto Starch Nanocrystals. *Biomacromolecules* **2007**, *8*, 2916−2927.

(29) Drelich, A.; Gomez, F.; Clausse, D.; Pezron, I. Evolution of Water-in-Oil Emulsions Stabilized with Solid Particles: Influence of Added Emulsifier. *Colloids Surf., A* **2010**, *365*, 171−177.

(30) Dee, G. T.; Sauer, B. B. The Molecular Weight and Temperature Dependence of Polymer Surface Tension: Comparison of Experiment with Interface Gradient Theory. *J. Colloid Interface Sci.* **1992**, *152*, 85−103.

(31) Dufresne, A. Processing of Polymer Nanocomposites Reinforced with Polysaccharide Nanocrystals. *Molecules* **2010**, *15*, 4111−4128.

(32) Halpin, J. C.; Kardos, J. L. Review: The Halpin-Tsai Equations. *Polym. Eng. Sci.* **1976**, *16*, 344−52.

(33) Fornes, T. D.; Paul, D. R. Modeling Properties of Nylon 6/Clay Nanocomposites Using Composite Theories. *Polymer* **2003**, *44*, 4993−5013.

(34) Wu, Y. P.; Jia, Q. X.; Yu, D. S.; Zhang, L. Q. Modeling Young's Modulus of Rubber−Clay Nanocomposites Using Composite Theories. *Polym. Test.* **2004**, *23*, 903−909.

(35) Boufi, S.; Kaddami, H.; Dufresne, A. Mechanical Performance and Transparency of Nanocellulose Reinforced Polymer Nanocomposites. *Macromol. Mater. Eng.* **2014**, *299*, 560−568.

(36) Althues, H.; Henle, J.; Kaskel, S. Functional Inorganic Nanofillers for Transparent Polymers. *Chem. Soc. Rev.* **2007**, *36*, 1454−1465.
(37) Landry, V.; Alemdar, A.; Blanchet, P. Nanocrystalline Cellulose: Morphological, Physical, and Mechanical Properties. *For. Prod. J.* **2011**, *61*, 104−112.
(38) www.acrylite-polymers.com.